Biomech Model Mechanobiol (2008) 7:405–416
DOI 10.1007/s10237-007-0104-z

ORIGINAL PAPER

A finite element model predicts the mechanotransduction response of tendon cells to cyclic tensile loading

Michael Lavagnino · Steven P. Arnoczky · Eugene Kepich · Oscar Caballero · Roger C. Haut

Received: 15 February 2007 / Accepted: 23 August 2007 / Published online: 28 September 2007

Abstract The importance of fluid-flow-induced shear stress and matrix-induced cell deformation in transmitting the global tendon load into a cellular mechanotransduction response is yet to be determined. A multiscale computational tendon model composed of both matrix and fluid phases was created to examine how global tendon loading may affect fluid-flow-induced shear stresses and membrane strains at the cellular level. The model was then used to develop a quantitative experiment to help understand the roles of membrane strains and fluid-induced shear stresses on the biological response of individual cells. The model was able to predict the global response of tendon to applied strain (stress, fluid exudation), as well as the associated cellular response of increased fluid-flow-induced shear stress with strain rate and matrix-induced cell deformation with strain amplitude. The model analysis, combined with the experimental results, demonstrated that both strain rate and strain amplitude are able to independently alter rat interstitial collagenase gene expression through increases in fluid-flow-induced shear stress and matrix-induced cell deformation, respectively.

M. Lavagnino (✉) · S. P. Arnoczky · O. Caballero
Laboratory for Comparative Orthopaedic Research,
College of Veterinary Medicine, Michigan State University,
East Lansing, MI 48824, USA
e-mail: lavagnin@cvm.msu.edu

E. Kepich · R. C. Haut
Orthopaedic Biomechanics Laboratories,
College of Osteopathic Medicine, Michigan State University,
East Lansing, MI 48824, USA

1 Introduction

Cells are known to respond to physical signals by way of a mechanotransduction tensegrity system, which connects the cell nucleus to the extracellular matrix through a cytoskeleton (Banes et al. 1995; Brown et al. 1998; Ingber 1997). Deformation of the cytoskeleton, via membrane anchored attachment proteins (integrins), or stimulation of other transmembrane proteins (G-protein receptors, receptor kinases, mitogen-activated protein kinases) (Wang 2006) initiates a cascade of gene expressions activating catabolic and/or anabolic cell responses (Lambert et al. 1992; Lavagnino and Arnoczky 2005; Mochitate et al. 1991). For tendons, the importance of physical stimuli in maintaining homeostasis has been well documented (Hannafin et al. 1995; Lavagnino et al. 2005; Woo et al. 1982; Yasuda and Hayashi 1999). Recent in vitro studies have shown that stress deprivation of tendon cells in situ results in an immediate up-regulation of rat interstitial collagenase mRNA expression (Arnoczky et al. 2004; Lavagnino et al. 2003). Conversely, application of static stress (Arnoczky et al. 2004) or cyclic strain (Lavagnino et al. 2003) has been shown to inhibit interstitial collagenase mRNA expression in this in vitro tendon model through a cytoskeletally based mechanism. While this gene inhibition has been shown to occur in an amplitude and frequency, dose-dependent manner (Lavagnino et al. 2003), the effect of cyclic loading rate on gene expression has not been explored.

Previous studies in bone have demonstrated that both matrix deformation and fluid flow are important regulators of gene expression (Han et al. 2004; Mullender et al. 2004; You et al. 2000). Application of tensile strain to tendons leads to a progressive loss of collagen crimp, an increase in fiber recruitment, and a subsequent deformation of the extracellular matrix (Hansen et al. 2002; Kastelic et al. 1980). Tendon

tensile strain has also been shown to modulate tendon cell deformation in a dose-dependent manner (Arnoczky et al. 2002a,b). Cellular deformation has also been implicated as a cell signaling mechanism in tendon cells through a calcium-based pathway (Arnoczky et al. 2007).

In addition to matrix deformation, experimental studies have demonstrated interstitial fluid flow in response to cyclic tensile loading of tendons (Hannafin and Arnoczky 1994; Helmer et al. 2006; Lanir et al. 1988). Fluid flow has been shown to control gene expression in a monolayer of tendon cells, presumably through a mechanotransduction mechanism, but without the significant calcium influx seen in deformed cells (Archambault et al. 2002). Therefore, it is possible that the dose-dependent inhibition of collagenase gene expression observed with increasing cyclic load amplitudes and/or frequencies may be related to concomitant increase in deformation and fluid-flow-induced shear stress on individual cells in the tendon (Lavagnino et al. 2003). However, the exact levels of fluid-induced shear stress on tendon cells in vivo have not been identified (Archambault et al. 2002).

While external loading is known to be an important regulator of bone metabolism, it has been suggested that fluid flow may actually play more of a role in matrix deformation in bone cell mechanotransduction (You et al. 2000). In tendons, a biphasic model has suggested the importance of distortional strain and hydrostatic stress as important mechanical stimuli regulating the composition of tendon and gene expression (Giori et al. 1993). This and other biphasic tendon models have successfully modeled global tendon properties in response to strain (Atkinson et al. 1997; Giori et al. 1993; Yin and Elliott 2004), but none have predicted local strains or fluid-induced shear stresses on the cell.

The mechanical response of tendon to load is determined by its solid (collagen matrix) and fluid components (Atkinson et al. 1997). Collagen fibers and their crimp formation are thought to play a significant role in determining the toe-in region of the nonlinear stress–strain response of tendon (Kastelic et al. 1980). Glycosaminoglycans have also been cited as strong determinants of mechanical properties due to their role in fibril–fibril binding (Redaelli et al. 2003) and their interaction with the fluid in the extracellular matrix (Robinson et al. 2004). The fluid content of a tendon, or its hydration, is known to alter the mechanical response of tendons to strain rate (Haut and Haut 1997). Although each of these components (extracellular matrix deformation and fluid flow) is known to play an important role in the mechanical response of tendon to load, their influence on cellular mechanotransduction is unknown.

Therefore, the purpose of this study was to create a multi-scale computational tendon model composed of both matrix and fluid phases to examine how global tendon loading may affect stresses and strains at the cellular level. *We hypothesized that mechanotransduction signaling in tendon cells can result from either increases in fluid- flow-induced shear stresses or membrane strains on the tendon cells.* The model was developed to study the results of previous experiments (Lavagnino et al. 2003) as well as to guide the development of new experiments to help understand the roles of membrane strains and fluid-induced shear stresses on the biological response of individual cells.

2 Model development

A multi-scale modeling approach was utilized in this study to help predict the levels of fluid-flow-induced shear stress on cells and cell membrane strain generated under various amplitudes and rates of global tendon loading.

2.1 Global model

The global model was based on the geometry and composition of a rat tail tendon (RTT). Tendons are made of three main components: type I collagen (70–80% of dry weight), an extrafibrillar matrix (proteoglycans, glycolipids, cells), and water (60–80% of wet weight) (Woo et al. 1997). Each of these components has mechanically significant functions in the response of tendon to load (Woo et al. 1997).

2.1.1 Collagen fibers

Collagen fibers have been previously modeled as linear elastic (Diamant et al. 1972; Kastelic et al. 1980; Stouffer et al. 1985), bilinear elastic (Belkoff and Haut 1992; Hurschler et al. 1997; Kwan and Woo 1989), and linear viscoelastic (Johnson et al. 1996; Wang et al. 1997; Wilson et al. 2004). To represent the nonlinear effects of collagen recruitment in the current model, collagen fibers were simulated using axially oriented nonlinear spring elements attached at the nodes of the matrix elements, similar to the model of Wilson et al. (1997). The tissue strain at which tendon fibers became uncrimped and began load bearing was assumed to vary linearly in the radial direction, with the largest strain required at the RTT center and the smallest strain at the outer boundary of the RTT (Hansen et al. 2002). The collagen fiber distribution in tendon was assumed to be uniform with no variation in collagen fiber density. Crosslinks between collagen fibers are formed by secondary collagen fibers (types VI, XII, XIV) and glycosaminoglycans. Although crosslinks are thought to play a role in the mechanical properties of tendon (Haut 1985; Puxkandl et al. 2002; Redaelli et al. 2003; Robinson et al. 2004), they are only indirectly (Poisson's ratio, low permeability) included in the current model.

2.1.2 Transversely isotropic matrix

Following the experimental demonstration of fluid exudation from tendon during cyclic tensile loading (Hannafin and Arnoczky 1994; Lanir et al. 1988), computational models have incorporated the effects of permeability and interstitial fluid flow (Adeeb et al. 2004; Atkinson et al. 1997; Butler et al. 1997; Chen et al. 1998; Yin and Elliott 2004). To adequately model fluid flow in the current model, the RTT matrix was assumed to be transversely isotropic in the fiber or two-axis direction, with a zero pore pressure enforced on the outer boundary to allow free fluid flow out of the tendon. The transversely isotropic model, with Poisson's ratio greater than 0.5, has been measured in ligament and shown to be necessary to generate fluid exudation in response to tensile load (Adeeb et al. 2004; Hewitt et al. 2001; Yin and Elliott 2004). Orthotropic materials may have higher Poisson's ratios (>0.5) than isotropic materials, as long as thermodynamic constraints are met (Adeeb et al. 2004). A Poisson's ratio greater than 0.5 is required for volume loss with uniaxial tension, and this volume loss is presumably due to fluid exudation from tendon (Yin and Elliott 2004). The high Poisson's ratio in tendon may be due to the organization of fibers and their crosslinks and not because of high Poisson's ratios of the individual tendon components (Adeeb et al. 2004). The Poisson's ratio in this model was chosen to reflect the fluid exudation effect of the whole tendon.

2.1.3 Tendon permeability

A major determinant of fluid flow is permeability, but the permeability of tendon is not known. However, it has been suggested that permeability is strain (Lai et al. 1981; Weiss and Maakestad 2006; Yin and Elliott 2004), porosity (Chen et al. 1998) and/or voids ratio (van der Voet 1997) dependent. Higher water content in the peripheral rim compared to the tendon core suggests that the porosity or voids ratio may also be depth dependent within a tendon (Wellen et al. 2005). The permeability in tendon is also believed to be anisotropic with a higher permeability along the fiber direction than across the fibers (Butler et al. 1997; Chen et al. 1998; Han et al. 2000). Although the directional dependence within tendon is known, the actual values are still in question. Therefore, for the current model, permeability and voids ratio were assumed to be uniform throughout the tendon.

2.2 Submodel

A submodeling function was utilized to provide the output from the global RTT model as boundary conditions in the cell model. The submodel consisted of an ovoid-shaped cell, a low-permeable cell membrane, pericellular and extracellular matrices, and nonlinear collagen fibers. Although tendon cells are often arranged in columns, the current model used a lone cell located on the outer boundary of the tendon. The outer boundary of the tendon was of interest, as cells in this area were assumed to be subject to the largest matrix deformations and fluid flows. In addition, a previous in situ study documented the cell nuclei deformation in this location following applied strain (Arnoczky et al. 2002a). The membrane of the cell was assumed to have a low permeability, thus diverting fluid to flow around and not through the cell (Ateshian et al. 2007). The pericellular matrix is surrounding the cell and cell membrane. The tendon pericellular matrix appears similar in composition to that of cartilage pericellular matrix in that they both contain versican and type VI collagen (Ritty et al. 2003). In cartilage, the pericellular matrix significantly alters the mechanical environment of the cell and thus plays a role in mechanotransduction (Guilak and Mow 2000). In addition, the submodel includes the transversly isotropic extracellular matrix and nonlinear collagen fibers as described for the global model.

3 Finite element method

3.1 Global model

The RTT was assumed to be cylindrically shaped with symmetry along the radial and axial directions. Thus, a global, poroelastic model of the RTT was created 20 mm long and 0.15 mm wide (Fig. 1). The RTT was divided into 300, 4-noded, axisymmetric elements (0.2 mm × 0.05 mm) using the commercial code ABAQUS 6.3 (ABAQUS, Inc. Providence, RI).

3.1.1 Collagen fibers

To represent the nonlinear effect of collagen recruitment, collagen fibers were simulated using axially oriented spring elements attached at the nodes of the matrix elements with a bilinear collagen spring stiffness of 0 N/mm during fiber straightening and 20 N/mm after fiber straightening (Wilson et al. 1997). The tendon deformation at which the fiber became uncrimped and began load bearing varied in the radial direction, with the largest strain required at the RTT center and the smallest strain at the outer boundary of the RTT (Fig. 2) (Hansen et al. 2002). A sensitivity analysis of the global tendon response to each parameter (data not shown) made it apparent that the collagen parameters (stiffness and uncrimping deformation) were dominant determinants of resultant force compared to matrix parameters. Therefore, these collagen parameters were manually adjusted to fit the experimental stress–strain curve of a tendon loaded to 3% strain at 6% strain/min. A constant fiber density of four columns of springs was used to mimic all collagen fibers.

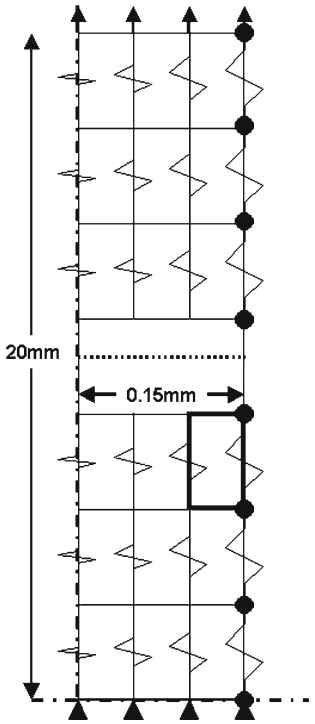

Fig. 1 Axisymmetric global poroelastic model of the rat tail tendon (20 mm × 0.15 mm), divided into 300 four-noded axisymmetric elements (0.2 mm × 0.05 mm) with radially variant nonlinear spring elements attached at the nodes of the matrix elements (springs), zero pore pressure on the outer boundary (*circles*), constrained at the tendon center (*triangles*), and loaded at the tendon end as per previous experimental conditions (*arrows*). The *darkened element boundary* indicates the location of the submodel

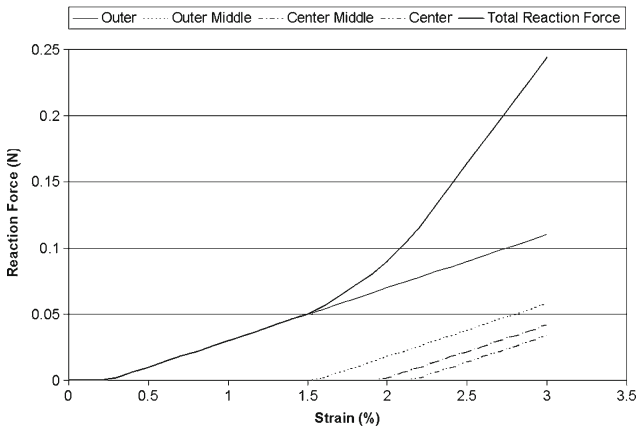

Fig. 2 Reaction force (*N*) plotted against strain (%) to show the radial variation in fiber recruitment from the outer boundary to the inner or center that predicts the nonlinear response of the global tendon

3.1.2 Transversely isotropic matrix

To adequately model fluid flow in the current model, the RTT matrix was assumed to be transversely isotropic in the fiber or two-axis direction. Material properties for the matrix were taken from the range of previous models and experiments on tendon and ligament (Table 1) (Adeeb et al. 2004; Atkinson et al. 1997; Gupta and Haut Donahue 2006; Haridas et al. 1999; Hewitt et al. 2001; Yin and Elliott 2004).

3.1.3 Boundary conditions

Boundary conditions on the global model included zero pore pressures on the outer boundary to allow free fluid flow out of the tendon (Fig. 1 circles) and constraint in the fiber direction at the RTT center to account for radial symmetry (Fig. 1 triangles). The RTT was elongated with an applied displacement to a peak strain in the first cycle at the same applied strain rate as previous experiments: 1% strain at 2% strain/min (0.017 Hz); 1% strain at 20% strain/min (0.17 Hz); 3% strain at 6% strain/min (0.017 Hz) (Fig. 1 arrows) (Lavagnino et al. 2003). Additionally, the model was also run in the current study at 3% strain and 2% strain/min (0.0056 Hz) to help understand the individual roles of fluid-induced shear stress and membrane strain on interstitial collagenase mRNA expression of tendon cells.

3.2 Submodel

The submodel was not axisymmetric and was located in the midportion along the length of the global model on the outer boundary (Fig. 1 darkened element) and composed of four-node bilinear displacement and pore pressure (CPE4P) elements.

3.2.1 Submodel components

A submodeling function was utilized to provide the output from the global RTT model (displacements, reaction forces, pore pressure) for boundary conditions in the cell model. The submodel was the size of the global element and it consisted of an ovoid-shaped cell, a low-permeable cell membrane, pericellular and extracellular matrices, and nonlinear collagen fibers (Fig. 3). The cell was chosen as an ovoid shape with a major axis length of 24 μm and minor axis length of 4 μm. The cell membrane in this model was used as a low-permeable barrier between the pericellular matrix and the cell to prevent fluid flow through the cell (Ateshian et al. 2007). The thickness of the membrane (500 nm) was chosen in an attempt to maintain a similar element size as the rest of the submodel and thus maintain numerical stability. This same cell membrane thickness has been previously used in other cell studies (Ateshian et al. 2006; Gupta and Haut Donahue 2006). Two limitations of this model associated with using a thicker membrane than normal (5–10 nm) include altered permeability and stiffness values. Having a thicker cell membrane may make the membrane stiffer and thus less deformable. The permeability defined for the cell membrane in this study is higher by a factor of 20 than

Table 1 Global matrix material properties

Parameters	E_2 (MPa)	$E_1 = E_3$ (MPa)	$\nu_{21} = \nu_{23}$	$\nu_{13} = \nu_{31}$	$G_{12} = G_{23}$ (MPa)	k (m^4/Ns)	Void ratio
Matrix	1.0	0.0457	1.7	0.7	0.1	3.08e-14	2.0
Reference range	0.0457–1.0	0.0457–1.0	0.7–2.73	0.3–0.9	0.157–5.0	5.5e-18–3.98e-14	1.0–2.33

(Adeeb et al. 2004; Atkinson et al. 1997; Gupta and Haut Donahue 2006; Haridas et al. 1999; Hewitt et al. 2001; Yin and Elliott 2004)

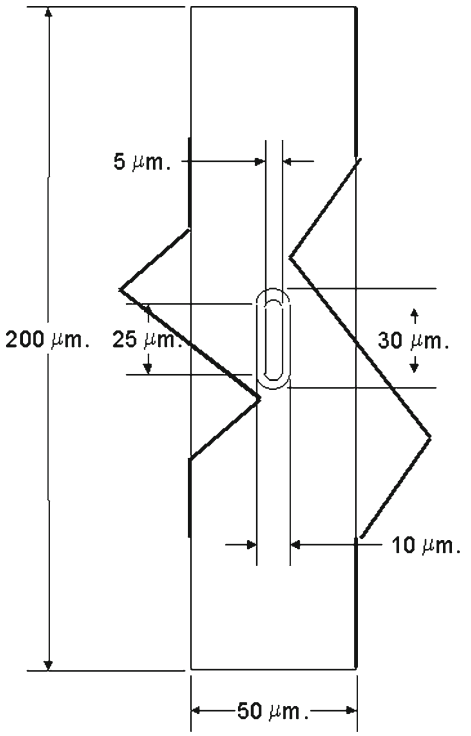

Fig. 3 Submodel of the rat tail tendon, the size of a global element, composed of an ovoid-shaped cell, cell membrane, pericellular matrix (PCM), extracellular matrix (ECM), and collagen fibers

that previously prescribed to represent the permeability for a 500 nm cell membrane (Ateshian et al. 2006). In taking the thickness of the cell membrane into effect we have potentially increased the cell stiffness and permeability and therefore predicted lower cell membrane deformation and fluid flow induced shear stress than using a normal membrane size (10 nm). Thus, using a larger membrane thickness to help maintain element stability in the submodel and altering its theoretical permeability, the cell membrane deformations and fluid-induced shear stresses were likely altered in the same direction to preserve the relationship and help validate the overall conclusions of this first study. These limitations must be investigated in future studies to further develop this mechanotransduction computational effort. Surrounding the cell and cell membrane is the pericellular matrix with a 2.5 μm thickness (Gupta and Haut Donahue 2006; Ritty et al. 2003). Linear poroelastic continuum elements were used to create the cell model with material properties taken from the

Table 2 Submodel material properties

Parameter	E (MPa)	υ	k (m^4/N s)	Void ratio
Pericellular matrix	1.0	0.490	3.924e-14	2.0
Cell membrane	1.0	0.490	4.905e-19	2.0
Cell	0.5	0.069	4.415e-14	2.0

(Guilak and Mow 2000; Gupta and Haut Donahue 2006)

range of previous models (Table 2) (Guilak and Mow 2000; Gupta and Haut Donahue 2006). The transversely isotropic extracellular matrix, as described for the global model, surrounds the pericellular matrix. Nonlinear springs, as collagen fibers, connect only the central and outside edges of the cell model (Fig. 3).

3.2.2 Submodel analysis

Coupled pore fluid diffusion and stress analysis were used to analyze the fluid flow velocities, stresses and strains within the model. Membrane strain was calculated by the change in the perimeter length divided by the original perimeter length as follows: $\varepsilon = \Delta\ell/\ell$. Fluid-flow-induced shear stress was calculated by the following equation $\tau = \mu\frac{\mathrm{d}u}{\mathrm{d}v}$, where μ was the viscosity of the fluid (0.001 Pa·s) and $\mathrm{d}u/\mathrm{d}v$ was the change in the fluid velocity perpendicular to the surface of the cell (Gupta and Haut Donahue 2006).

4 Experimental methods

To compare the predicted cellular stresses and strains to the interstitial collagenase mRNA inhibition of tendon cells in situ, the following in vitro experiment was performed.

4.1 Cyclic tensile loading

After Institutional Animal Care and Use Committee approval was granted, rat tail tendons were harvested from adult Sprague–Dawley rats immediately after killing. Using a sterile scalpel blade, the tail was cut between coccygeal vertebrae at both the base and at the distal tip of the tail for a total length of approximately 120 mm. Tendons were gently teased from the distal portion of each tail with forceps and maintained in DMEM media supplemented with 10%

FBS, antibiotic/antimycotic solution and ascorbate incubated at 37°C and 10% CO_2. The rat tail tendons were divided into six groups as follows: Group A: 1% cyclic strain at 2% strain/min (0.017 Hz) for 24 h; Group B: 1% cyclic strain at 20% strain/min (0.17 Hz) for 24 h; Group C: 3% cyclic strain at 6% strain/min (0.017 Hz) for 24 h; Group D: 3% cyclic strain at 2% strain/min (0.0056 Hz) for 24 h; Group E: stress-deprived for 24 h; Group F: fresh (0 h) control. All experimental input parameters, except Group D, were the same as in previous studies (Lavagnino et al. 2003). Stress-deprived tendons were maintained in a culture dish in complete media under tissue culture conditions. Cyclic strain was applied to tendons in complete media under tissue culture conditions using a custom-made, computer controlled, motor-driven device (Lavagnino et al. 2003). While in the previous study northern blots were used to show alterations in collagenase expression with various global loading parameters, in the current study matrix metalloproteinase (MMP)-13 (rat interstitial collagenase) mRNA expression was quantified using quantitative real-time polymerase chain reaction (Q-PCR).

4.2 Quantitative polymerase chain reaction

At the end of each experimental period, ten tendons from each group were placed in 1.0 ml of RNAlater^{TM} (Qiagen, Valencia, CA) for a period of at least 24 h at 4°C before processing. Total RNA was then extracted using the Qiagen RNEasy Kit (Valencia, CA) with the protocol provided for fibrous tissues. RNA (200–400 ng), once concentrations were normalized, was converted into cDNA using the Invitrogen SuperScript III Reverse Transcription system (Carlsbad, CA). Real time quantitative PCR was performed using the TaqMan Gene Expression Assay from Applied Biosystems (ABI, Foster City, CA). Samples were run in a 96-well plate (20 µl final volume per reaction) on an ABI 7500-Fast Q-PCR apparatus. The endogenous control used for all Q-PCR experiments was 18 s rRNA. Results were analyzed using the Sequence Detection System software available from ABI. TaqMan probe and primer sets were obtained for MMP-13 (Rn01448197_m1) and 18 s rRNA (Hs99999901_s1) from ABI's Gene Expression Assay database (http://allgenes.com).

5 Results

5.1 Finite element results

The global model analysis closely predicted the nonlinear stress–strain response of the tendon to 3% strain at 6% strain/min (Fig. 4). In addition, the global model also indicated fluid flow in a radial direction leaving the tendon during tensile stretch (Fig. 5). On the submodel level, this fluid was predicted to flow around the cell with the highest velocity occurring at the cell poles (Fig. 6).

The tendon model predicted that increasing both the global strain rate (2–6% strain/min) and strain amplitude (1–3%) (group A versus C) would result in an increase in both the

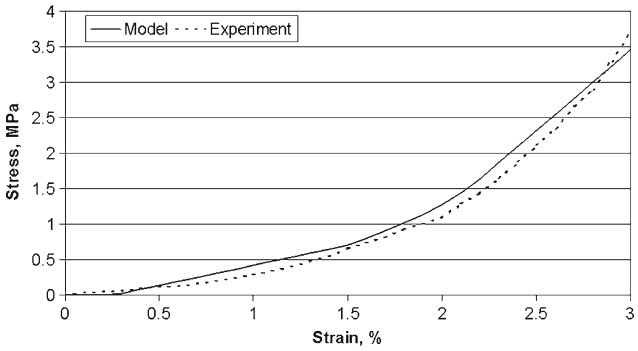

Fig. 4 Comparison of tendon model to actual tendon stress–strain response (3% strain at 6% strain/min)

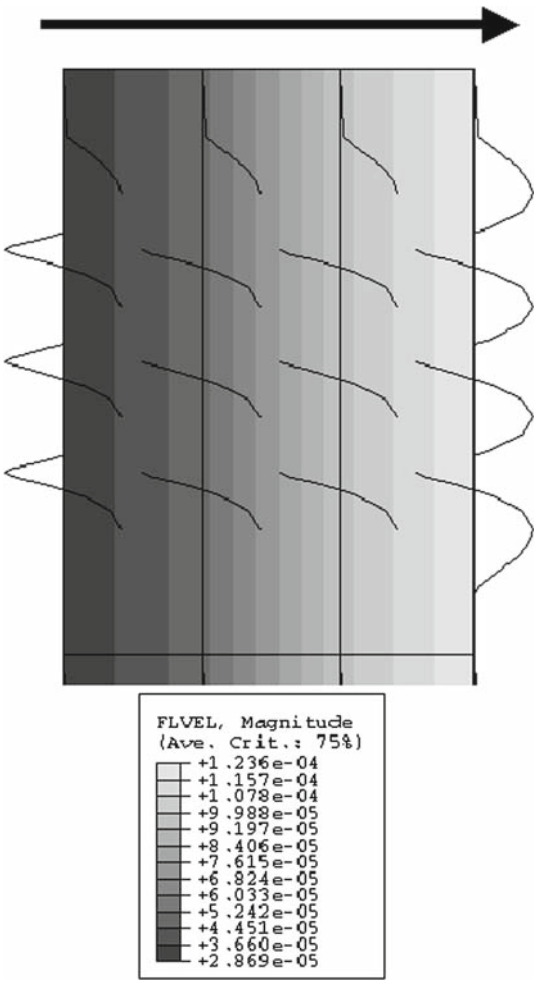

Fig. 5 Plot of the fluid velocity magnitude (mm/s) showing fluid flow in the positive direction (*arrow*) out of the tendon (3% strain at 6% strain/min). The *curved lines* (springs) represent the collagen fibers

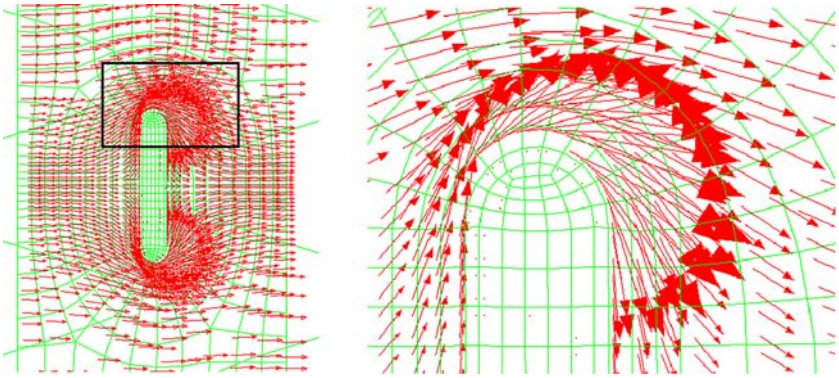

Fig. 6 Plots of the fluid velocity resultant around the cell and out of the tendon (3% strain at 6% strain/min)

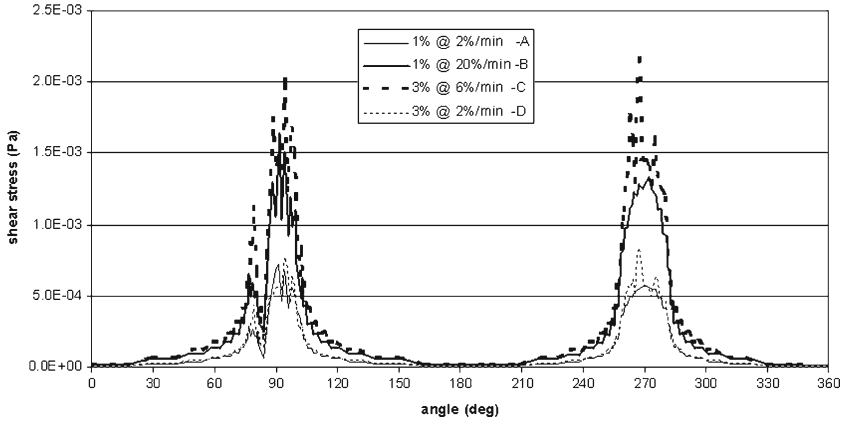

Fig. 7 Graph of shear–stress induced by fluid flow. Note the marked increase in at the polar ends of the cell

Table 3 Global model and submodel strain and shear stress values

	Group A	Group B	Group C	Group D
Global model strain (%)	1.00	1.00	3.00	3.00
Global model strain rate (% strain/min)	2.00	20.0	6.00	2.00
Cell membrane strain (%)	1.26	1.33	3.67	3.97
Maximum shear stress at 270° (mPa)	0.414	0.927	1.004	0.409
Average shear stress (mPa)	0.157	0.346	0.459	0.179
Collagenase expression (Lavagnino et al. 2003)	Inhibited	Eliminated	Eliminated	NA

maximum shear stress (142%) and cell membrane strain (191%) (Fig. 7; Table 3). With an increase in the applied strain rate from 2 to 20% strain/min at 1% global model strain (group A versus B), the model predicted a corresponding 124% increase in the maximum localized shear stress at the cell poles, but only a modest (5%) increase in cell membrane strain (Fig. 7; Table 3). In contrast, the theoretical responses of the tendon model for inputs of 1% strain at 20% strain/min (group B) versus 3% strain at 6% strain/min (group C) generated similar maximum shear stress values (8% difference). However, the cell membrane strain levels were increased by 175%. The model was then exercised in an attempt to define an experiment to further explore the effects of membrane strain and shear stress. For a 3% strain at 2% strain/min (group D), the model predicted a cell membrane strain within 8% of group C, with a maximum shear stress that was 145% less than group C (Fig. 7; Table 3).

5.2 Q-PCR results

The Q-PCR results from each group of tendons suggested direct correlations could be established between the levels of membrane strain and shear stress predicted in the model and the inhibition of collagenase mRNA. These data were calculated relative to the fresh control (0 h) sample (Fig. 8). Tendon cells exposed to a higher global strain rate and strain amplitude (group A vs C), expressed a significantly reduced amount of rat interstitial collagenase mRNA (Fig. 8; Table 3). Increasing the global strain rate from 2 to 20% strain/min at 1% global model strain (group A vs B) also significantly

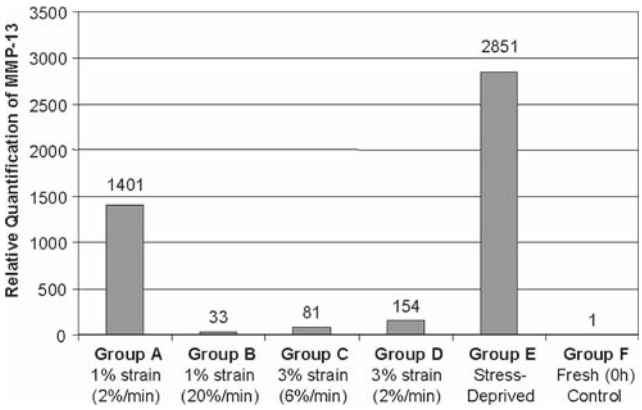

Fig. 8 Gene expression levels of rat interstitial collagenase (MMP-13) as determined by real-time Quantitative PCR. All experimental samples were quantified relative to the fresh (0 h) control

reduced this expression. On the other hand, increasing the amplitude of global strain (1–3%), with a reduction of global strain rate from 20 to 6% per minute (group B vs C), had little effect on the expression of rat interstitial collagenase mRNA expression (Fig. 8; Table 3). These data were thus suggestive that enhanced shear stress, rather than increased cell membrane strain was primarily responsible for inhibition of collagenase expression. Furthermore, it was seen that in comparing the results of group C to D, where the fluid-induced shear stress on the cell was significantly reduced at 3% strain, the expression of rat interstitial collagenase mRNA was increased. Alternatively, if the Q-PCR results of group A versus D were compared, the collagenase expression was significantly reduced (Fig. 8). This biological response of the tendon was associated with a theoretical increase in cell membrane strain and little change in the fluid-induced shear stress on the cell (Table 3).

6 Discussion

The results of the initial study showed a strong association between the amount of fluid-flow-induced shear stress on the cell and the inhibition of collagenase mRNA expression, regardless of cell strain. The importance of fluid-flow-induced shear stress was confirmed when the additional boundary condition was predicted and showed that a decrease in shear stress with the same cell membrane strain resulted in less collagenase mRNA inhibition (3% strain at 6% strain/min [C] versus 3% strain at 2% strain/min [D]). However, the additional boundary condition also showed that increasing the membrane strain at similar low fluid-induced shear stress also resulted in a decrease in collagenase mRNA expression (1% strain at 2% strain/min [A] versus 3% strain at 2% strain/min [D]). Therefore, increased fluid-flow-induced shear stress alone and cell membrane strain alone were shown to inhibit the expression of rat interstitial collagenase mRNA. Thus, the results of this study confirm our hypothesis that fluid-flow-induced shear stresses and matrix-induced cell deformation are able to alter catabolic gene expression, presumably through a mechanotransduction pathway.

The interstitial fluid flow and extrusion out of tendon predicted by the model have been documented to occur in tendon following application of static and cyclic tensile loading (Hannafin and Arnoczky 1994; Helmer et al. 2006; Lanir et al. 1988) although the exact amount of fluid exuded per stretch remains unknown. The increased fluid flow predicted around the cell with increased loading rate may explain why collagenase mRNA expression decreases (Lavagnino et al. 2003). Similar to matrix-induced cell deformation, fluid flow has also been suggested to affect cell function and gene expression; however, the method of action is yet to be determined (Hannafin and Arnoczky 1994). A previous study has shown that the fluid flow induced by cyclic or static load did not alter the diffusion of low-molecular weight solutes compared to unloaded controls (Hannafin and Arnoczky 1994). These conclusions suggested that any biological benefit of cyclic loading (and resultant fluid flow) is not probably due to an increase in cell nutrition (Hannafin and Arnoczky 1994). Fluid flow, as suggested in bone, may alter gene expression as it induces a drag gradient on the pericellular matrix fibers (Han et al. 2004). The drag gradient on the pericellular fibers, which are connected to the cell membrane, in turn creates a drag force on the cell, thereby creating strain amplification from fluid (Han et al. 2004). While the current model does not include pericellular matrix fibers, the increased fluid velocity with increased strain rate suggests that a similar phenomenon could occur in tendons.

An increase in fluid-induced shear stress on the cell could also explain the decreased collagenase expression with increased fluid flow. Fluid flow induces shear stress on the cell membrane and can mechanically stimulate cells to alter their gene expression (Archambault et al. 2002; Jin et al. 2000; Ng et al. 2005; You et al. 2000). The current model predicts that cyclic strain at low rate and amplitude results in an average shear stress of 0.157 mPa. The magnitude of the shear stress increases significantly with increased rate (0.346 mPa) or amplitude and rate (0.459 mPa) corresponding with the inhibition of collagenase mRNA expression. While the amount of fluid-induced shear stress on tendon cells under physiological conditions in vivo is unknown, both cartilage and tendon models have suggested that interstitial fluid flow may be in the range of 54 nm/s to 10 μm/s, resulting in fluid-induced shear of ~65 mPa (Ateshian et al. 2007; Frank and Grodzinsky 1987; Ng et al. 2005). In a low flow (6.3 μm/s) study, myofibroblasts seeded in a 3D collagen gel scaffold were subjected to an estimated average fluid shear stress on the cells that varied between 15 and 33 mPa, which were considered superphysiological (Ng et al. 2005). These values of

shear stress from interstitial flow have been shown to strongly induce an anabolic response by fibroblasts (Ng et al. 2005). Therefore, the levels of fluid-induced shear stress predicted in this study appear to sufficiently approximate the values needed to inhibit catabolic gene expression. Previous studies have applied no load (stress-deprivation) (Arnoczky et al. 2004; Lavagnino et al. 2003) or much higher levels of fluid-induced shear stress to cells (0.1–2.5 Pa) to induce a catabolic response (Archambault et al. 2002; Jin et al. 2000). Although suggested by the current study, additional studies are needed to determine whether a range of shear stress may exist that result in a homeostatic mechanobiological response, where an imbalance above or below that shear stress range would result in a catabolic response.

The strain magnitude experienced by rat tail tendons in vivo is unknown; however, the model was able to predict the cell membrane deformation and the corresponding gene response to the in vitro applied loads. The matrix-induced cell deformation predicted by the model has also been documented to occur in tendon following application of static tensile load (Arnoczky et al. 2002a; Hansen et al. 2002; Kastelic et al. 1980). In addition, static tendon load is known to correlate with nuclear strain (Arnoczky et al. 2002a) and has been shown to have a dose-dependent effect on gene expression due to cytoskeletal deformation (Arnoczky et al. 2004). Cell deformation and the resulting alterations in the cytoskeleton are key components in the mechanotransduction response(s) of cells (Banes et al. 1995). The dose-dependent inhibition of rat interstitial collagenase mRNA with cyclic strain amplitude shown in this study continues to support the mechanosensitive response of cells to deformation.

Therefore, both strain rate and strain amplitude appear to play a role in altering cellular gene expression in tendon. This mechanoresponsiveness of tendon cells is vital to maintain tendon homeostasis (Lavagnino and Arnoczky 2005). The importance of both the fluid and solid components in transmitting mechanical signals to cells has been suggested in other biphasic tissue studies (Guilak and Mow 2000; Gupta and Haut Donahue 2006; You et al. 2000). Although this cellular response to global load has been studied in cartilage and meniscus (Guilak and Mow 2000; Gupta and Haut Donahue 2006), this is the first study to predict the mechanical environment of tendon cells to tensile loading.

Although the current study suggests that interstitial collagenase gene expression has both rate and amplitude dose dependence, it was not possible to determine whether rate or amplitude plays a more significant role in maintaining homeostasis. Studies in bone cells suggest fluid flow plays a significantly greater role than substrate deformation in activating gene expression (You et al. 2000). One reason for this dichotomy may be due to how fluid-shear and matrix strains play a role in mechanotransduction. With tendon cell deformation, calcium influx is a first and primary responder prior to alterations in gene expression (Archambault et al. 2002). However, even at high fluid-shear rates and with the induction of collagenase, there is no significant calcium influx in tendon cells (Archambault et al. 2002). Thus, gene expression may be activated through different mechanotransduction mechanisms (kinases, stretch-activated ion channels) depending on the mechanical signal experienced by the cell (Archambault et al. 2002). Indeed, kinases are cell membrane proteins that are phosphorylated when subjected to cyclic stretching or shear stress (Arnoczky et al. 2002b; Iwasaki et al. 2000; Wang 2006).

The current computational model uses continuum mechanics to determine membrane deformations and fluid-flow-induced shear stresses on the cell. The cell is a discrete structural entity composed of many individual parts (cytoskeleton, nucleus, cytoplasm, organelles, cellular membrane, etc.) that may each play a role in mechanotransduction. Therefore, it was assumed that strains and stresses on the cell continuum would translate into strains and stresses on the cellular components, thus leading to a biological response.

A limitation of this study is that permeability is assumed constant throughout the tendon. Previous computational models and experiments have suggested that tendon permeability is anisotropic and strain dependent (Butler et al. 1997; Chen et al. 1998; Han et al. 2000; Yin and Elliott 2004; You et al. 2000). The use of constant permeability may limit the model from determining strain-dependent changes in fluid flow that could help explain the weaker rate dependence of interstitial collagenase mRNA expression at higher strain amplitudes seen in this study. Future studies should investigate how the anisotropic, strain-dependent permeability of tendon would affect the magnitude of fluid flow around the cells.

Permeability was further investigated over the range of values seen in the literature (data not shown). The results of this analysis showed that the reduced permeability significantly lowered the fluid-flow induced shear stress predicted on the cell, while only modestly lowering the cell membrane strain. However, this change in permeability did not alter the overall relationship of shear stress between groups. The permeability of the PCM would also seem to have a potentially important impact on the shear stress developed on the cell membrane from fluid flow. Thus, this additional analysis demonstrates the importance of determining the material properties of tendon both at the global and cellular level to accurately model tendon mechanical signals on the cell.

The current model assumes that the collagen fibers act as springs and therefore the model does not allow for load transfer between fibers or between the fibers and the matrix and cell. Collagen crosslinking with both covalent (Haut 1985) and GAG bonds (Redaelli et al. 2003; Scott 2003) are thought to play an important role in tendon mechanics. A recent study, however, does not support the theory that sulfated GAG

cross-links influence continuum-level mechanical behavior during quasi-static tensile loading (Lujan et al. 2007). However, the dermatin sulfate may still contribute to the viscoelastic response when other loading rates or protocols are used (Lujan et al. 2007). The fluid content of tendon determines the strain-rate-sensitive stiffness of tendon (Haut and Haut 1997). Therefore, although the crosslinking effect of GAGs may not be as important as previously theorized, the water content of tendon due to the GAG concentration may still contribute to both the mechanical properties and the cell response of tendons. Therefore, although the collagen fibers as springs may be able to closely predict the global tendon response, they remain a limitation through their inability to transfer load to the matrix and thus alter the fluid response of the tendon upon loading.

The cellular stresses and strains in this study are only evaluated following the global applied displacement to peak strain in the first cycle. Therefore, the correlations between global loading, cell loading, and the corresponding gene expression are all based on this one time point. The peak strain of the first cycle was assumed to validly represent the peak values of deformation and shear stress experienced by the cell. However, this assumption is another limitation of this study and additional studies are required to determine how tendon hysterisis and/or stress relaxation may affect mechanical signals at the cellular level over a 24-h time period of cyclic strain.

In conclusion, the model was able to predict the global response of tendon to applied strain (stress, fluid exudation), as well as the associated cellular response of increased fluid-flow-induced shear stress with strain rate and matrix-induced cell deformation with strain amplitude. The model analysis, combined with the experimental results, showed that both strain rate and strain amplitude are able to independently alter catabolic gene expression through increases in fluid-flow-induced shear stress and matrix-induced cell deformation, respectively. Although shear stress and cell deformation appear to alter gene expression through mechanotransduction pathways, additional studies are required to separate the importance of these mechanical factors in homeostasis, injury, or rehabilitation.

References

Adeeb S, Ali A, Shrive N, Frank C, Smith D (2004) Modelling the behaviour of ligaments: a technical note. Comput Methods Biomech Biomed Eng 7:33–42

Archambault JM, Elfervig-Wall MK, Tsuzaki M, Herzog W, Banes AJ (2002) Rabbit tendon cells produce MMP-3 in response to fluid flow without significant calcium transients. J Biomech 35: 303–309

Arnoczky SP, Lavagnino M, Whallon JH, Hoonjan A (2002a) In situ cell nucleus deformation in tendons under tensile load; a morphological analysis using confocal laser microscopy. J Orthop Res 20:29–35

Arnoczky SP, Tian T, Lavagnino M, Gardner K, Schuler P, Morse P (2002b) Activation of stress-activated protein kinases (SAPK) in tendon cells following cyclic strain: the effects of strain frequency, strain magnitude, and cytosolic calcium. J Orthop Res 20:947–952

Arnoczky SP, Tian T, Lavagnino M, Gardner K (2004) Ex vivo static tensile loading inhibits MMP-1 expression in rat tail tendon cells through a cytoskeletally based mechanotransduction mechanism. J Orthop Res 22:328–333

Arnoczky SP, Lavagnino M, Egerbacher M (2007) The response of tendon cells to changing loads: implications in the etiopathogenesis of tendinopathy. In: Woo SL, Renstrom P, Arnoczky SP (eds) Tendinopathy in athletes. Blackwell, Oxford, pp 46–59

Ateshian GA, Likhitpanichkul M, Hung CT (2006) A mixture theory analysis for passive transport in osmotic loading of cells. J Biomech 39:464–475

Ateshian GA, Costa KD, Hung CT (2007) A theoretical analysis of water transport through chondrocytes. Biomech Model Mechanobiol 6:91–101

Atkinson TS, Haut RC, Altiero NJ (1997) A poroelastic model that predicts some phenomenological responses of ligaments and tendons. J Biomech Eng 119:400–405

Banes AJ, Tsuzaki M, Yamamoto J, Fischer T, Brigman B, Brown T, Miller L (1995) Mechanoreception at the cellular level: the detection, interpretation, and diversity of responses to mechanical signals. Biochem Cell Biol 73:349–365

Belkoff SM, Haut RC (1992) Microstructurally based model analysis of gamma-irradiated tendon allografts. J Orthop Res 10:461–464

Brown RA, Prajapati R, McGrouther DA, Yannas IV, Eastwood M (1998) Tensional homeostasis in dermal fibroblasts: mechanical responses to mechanical loading in three-dimensional substrates. J Cell Physiol 175:323–332

Butler SL, Kohles SS, Thielke RJ, Chen C, Vanderby R Jr (1997) Interstitial fluid flow in tendons or ligaments: a porous medium finite element simulation. Med Biol Eng Comput 35:742–746

Chen CT, Malkus DS, Vanderby R Jr (1998) A fiber matrix model for interstitial fluid flow and permeability in ligaments and tendons. Biorheology 35:103–118

Diamant J, Keller A, Baer E, Litt M, Arridge RG (1972) Collagen; ultrastructure and its relation to mechanical properties as a function of ageing. Proc R Soc Lond B Biol Sci 180:293–315

Frank EH, Grodzinsky AJ (1987) Cartilage electromechanics—II. A continuum model of cartilage electrokinetics and correlation with experiments. J Biomech 20:629–639

Giori NJ, Beaupre GS, Carter DR (1993) Cellular shape and pressure may mediate mechanical control of tissue composition in tendons. J Orthop Res 11:581–591

Guilak F, Mow VC (2000) The mechanical environment of the chondrocyte: a biphasic finite element model of cell–matrix interactions in articular cartilage. J Biomech 33:1663–1673

Gupta T, Haut Donahue TL (2006) Role of cell location and morphology in the mechanical environment around meniscal cells. Acta Biomater 2:483–492

Han S, Gemmell SJ, Helmer KG, Grigg P, Wellen JW, Hoffman AH, Sotak CH (2000) Changes in ADC caused by tensile loading of rabbit achilles tendon: evidence for water transport. J Magn Reson 144:217–227

Han Y, Cowin SC, Schaffler MB, Weinbaum S (2004) Mechanotransduction and strain amplification in osteocyte cell processes. Proc Natl Acad Sci USA 101:16689–16694

Hannafin JA, Arnoczky SP (1994) Effect of cyclic and static tensile loading on water content and solute diffusion in canine flexor tendons: an in vitro study. J Orthop Res 12:350–356

Hannafin JA, Arnoczky SP, Hoonjan A, Torzilli PA (1995) Effect of stress deprivation and cyclic tensile loading on the material and morphologic properties of canine flexor digitorum profundus tendon: an in vitro study. J Orthop Res 13:907–914

Hansen KA, Weiss JA, Barton JK (2002a) Recruitment of tendon crimp with applied tensile strain. J Biomech Eng 124:72–77

Haridas B, Butler DL, Malaviya P, Boivin G, Awad H, Smith F (1999) Transversely isotropic poroelastic finite element simulations of the intact and surgically translocated rabbit flexor tendon. Proceedings of the 1999 ASME Summer Bioengineering Conference

Haut RC (1985) The effect of a lathyritic diet on the sensitivity of tendon to strain rate. J Biomech Eng 107:166–174

Haut TL, Haut RC (1997) The state of tissue hydration determines the strain-rate-sensitive stiffness of human patellar tendon. J Biomech 30:79–81

Helmer KG, Nair G, Cannella M, Grigg P (2006) Water movement in tendon in response to a repeated static tensile load using one-dimensional magnetic resonance imaging. J Biomech Eng 128:733–741

Hewitt J, Guilak F, Glisson R, Vail TP (2001) Regional material properties of the human hip joint capsule ligaments. J Orthop Res 19:359–364

Hurschler C, Loitz-Ramage B, Vanderby R Jr (1997) A structurally based stress-stretch relationship for tendon and ligament. J Biomech Eng 119:392–399

Ingber DE (1997) Tensegrity: the architectural basis of cellular mechanotransduction. Annu Rev Physiol 59:575–599

Iwasaki H, Eguchi S, Ueno H, Marumo F, Hirata Y (2000) Mechanical stretch stimulates growth of vascular smooth muscle cells via epidermal growth factor receptor. Am J Physiol Heart Circ Physiol 278:H521–529

Jin G, Sah RL, Li YS, Lotz M, Shyy JY, Chien S (2000) Biomechanical regulation of matrix metalloproteinase-9 in cultured chondrocytes. J Orthop Res 18:899–908

Johnson GA, Livesay GA, Woo SL, Rajagopal KR (1996) A single integral finite strain viscoelastic model of ligaments and tendons. J Biomech Eng 118:221–226

Kastelic J, Palley I, Baer E (1980) A structural mechanical model for tendon crimping. J Biomech 13:887–893

Kwan MK, Woo SL (1989) A structural model to describe the nonlinear stress-strain behavior for parallel-fibered collagenous tissues. J Biomech Eng 111:361–363

Lai WM, Mow VC, Roth V (1981) Effects of nonlinear strain-dependent permeability and rate of compression on the stress behavior of articular cartilage. J Biomech Eng 103:61–66

Lambert CA, Soudant EP, Nusgens BV, Lapiere CM (1992) Pretranslational regulation of extracellular matrix macromolecules and collagenase expression in fibroblasts by mechanical forces. Lab Invest 66:444–451

Lanir Y, Salant EL, Foux A (1988) Physico-chemical and microstructural changes in collagen fiber bundles following stretch in-vitro. Biorheology 25:591–603

Lavagnino M, Arnoczky SP (2005) In vitro alterations in cytoskeletal tensional homeostasis control gene expression in tendon cells. J Orthop Res 23:1211–1218

Lavagnino M, Arnoczky SP, Tian T, Vaupel Z (2003) Effect of amplitude and frequency of cyclic tensile strain on the inhibition of MMP-1 mRNA expression in tendon cells: an in vitro study. Connect Tissue Res 44:181–187

Lavagnino M, Arnoczky SP, Frank K, Tian T (2005) Collagen fibril diameter distribution does not reflect changes in the mechanical properties of in vitro stress-deprived tendons. J Biomech 38: 69–75

Lujan TJ, Underwood CJ, Henninger HB, Thompson BM, Weiss JA (2007) Effect of dermatan sulfate glycosaminoglycans on the quasi-static material properties of the human medial collateral ligament. J Orthop Res 25:894–903

Mochitate K, Pawelek P, Grinnell F (1991) Stress relaxation of contracted collagen gels: disruption of actin filament bundles, release of cell surface fibronectin, and down-regulation of DNA and protein synthesis. Exp Cell Res 193:198–207

Mullender M, El Haj AJ, Yang Y, van Duin MA, Burger EH, Klein-Nulend J (2004) Mechanotransduction of bone cells in vitro: mechanobiology of bone tissue. Med Biol Eng Comput 42:14–21

Ng CP, Hinz B, Swartz MA (2005) Interstitial fluid flow induces myofibroblast differentiation and collagen alignment in vitro. J Cell Sci 118:4731–4739

Puxkandl R, Zizak I, Paris O, Keckes J, Tesch W, Bernstorff S, Purslow P, Fratzl P (2002) Viscoelastic properties of collagen: synchrotron radiation investigations and structural model. Philos Trans R Soc Lond B Biol Sci 357:191–197

Redaelli A, Vesentini S, Soncini M, Vena P, Mantero S, Montevecchi FM (2003) Possible role of decorin glycosaminoglycans in fibril to fibril force transfer in relative mature tendons—a computational study from molecular to microstructural level. J Biomech 36:1555–1569

Ritty TM, Roth R, Heuser JE (2003) Tendon cell array isolation reveals a previously unknown fibrillin-2-containing macromolecular assembly. Structure (Camb) 11:1179–1188

Robinson PS, Lin TW, Jawad AF, Iozzo RV, Soslowsky LJ (2004) Investigating tendon fascicle structure-function relationships in a transgenic-age mouse model using multiple regression models. Ann Biomed Eng 32:924–931

Scott JE (2003) Elasticity in extracellular matrix 'shape modules' of tendon, cartilage, etc. A sliding proteoglycan-filament model. J Physiol 553:335–343

Stouffer DC, Butler DL, Hosny D (1985) The relationship between crimp pattern and mechanical response of human patellar tendon–bone units. J Biomech Eng 107:158–165

van der Voet A (1997) A comparison of finite element codes for the solution of biphasic poroelastic problems. Proc Inst Mech Eng 211:209–211

Wang JH (2006) Mechanobiology of tendon. J Biomech 39:1563–1582

Wang JL, Parnianpour M, Shirazi-Adl A, Engin AE (1997) Failure criterion of collagen fiber: viscoelastic behavior simulated by using load control data. Theory Appl Fracture Mechs 27:1–12

Weiss JA, Maakestad BJ (2006) Permeability of human medial collateral ligament in compression transverse to the collagen fiber direction. J Biomech 39:276–283

Wellen J, Helmer KG, Grigg P, Sotak CH (2005) Spatial characterization of T1 and T2 relaxation times and the water apparent diffusion coefficient in rabbit Achilles tendon subjected to tensile loading. Magn Reson Med 53:535–544

Wilson A, Shelton F, Chaput C, Frank C, Butler D, Shrive N (1997) The shear behaviour of the rabbit medial collateral ligament. Med Eng Phys 19:652–657

Wilson W, van Donkelaar CC, van Rietbergen B, Ito K, Huiskes R (2004) Stresses in the local collagen network of articular cartilage: a poroviscoelastic fibril-reinforced finite element study. J Biomech 37:357–366

Woo SL, Gomez MA, Woo YK, Akeson WH (1982) Mechanical properties of tendons and ligaments. II. The relationships of immobilization and exercise on tissue remodeling. Biorheology 19: 397–408

Woo SL, Livesay GA, Runco TJ, Young EP (1997) Structure and function of tendons and ligaments. In: Mow VC, Hayes WC (eds) Basic orthopaedic biomechanics. Lippincott-raven, Philadelphia, pp 209–251

Yasuda K, Hayashi K (1999) Changes in biomechanical properties of tendons and ligaments from joint disuse. Osteoarthritis Cartilage 7:122–129

Yin L, Elliott DM (2004) A biphasic and transversely isotropic mechanical model for tendon: application to mouse tail fascicles in uniaxial tension. J Biomech 37:907–916

You J, Yellowley CE, Donahue HJ, Zhang Y, Chen Q, Jacobs CR (2000) Substrate deformation levels associated with routine physical activity are less stimulatory to bone cells relative to loading-induced oscillatory fluid flow. J Biomech Eng 122:387–393